

1
2
3
4
5
6
7
8
9
10
11
12
13
14
15
16
17

LPJ-GM 1.0: Simulating migration efficiently in a dynamic vegetation model

Lehsten, Veiko^{a,b}, Mischurow, Michael^b, Lindström, Erik^c, Lehsten, Dörte^b, Lischke, Heike^a

^a Dynamic Macroecology/Land change science, Swiss Federal Institute for Forest, Snow and Landscape Research WSL, Birmensdorf, Switzerland

^b Department of Physical Geography and Ecosystem Science, Lund University, Lund, Sweden

^c Centre for Mathematical Sciences, Department for Mathematics Lund University, Lund, Sweden

* Corresponding author: veiko.lehsten@gmail.com

18 **Abstract**

19 Dynamic global vegetation models are a common tool to assess the effect of climate and land use
20 change on vegetation. Though most applications of dynamic global vegetation models use plant
21 functional types, some also simulate species occurrences. While the current development aims to
22 include more processes, e.g. the nitrogen cycle, the models still typically assume an ample seed supply
23 allowing all species to establish once the climate conditions are suitable. Pollen studies have shown
24 that a number of plant species lag behind in occupying climatological suitable areas (e.g. after a
25 change in the climate) as they need to arrive at and establish in the newly suitable areas. Previous
26 attempts to implement migration in dynamic vegetation models have allowed simulating either only
27 small areas or have been implemented as post process, not allowing for feedbacks within the
28 vegetation. Here we present two novel methods simulating migrating and interacting tree species
29 which have the potential to be used for simulations of large areas. Both distribute seeds between grid
30 cells leading to individual establishment. The first method uses an approach based on Fast Fourier
31 Transforms while in the second approach we iteratively shift the seed production matrix and disperse
32 seeds with a given probability. While the former method is computationally faster, it does not allow
33 for modification of the seed dispersal kernel parameters with respect to terrain features, which the
34 latter method allows.

35 We evaluate the increase in computational demand of both methods. Since dispersal acts at a scale no
36 larger than 1 km, all dispersal simulations need to be performed at maximum at that scale. However,
37 with the current available computational power it is not feasible to simulate the local vegetation
38 dynamics of a large area at that scale. We present an option to decrease the required computational
39 costs, reducing the number of grid cells where the local dynamics is simulated only along migration
40 transects. Evaluation of species patterns and migration speeds shows that the simulation along
41 transects reduces the migration speed, and both methods applied, on the transects, produce reasonable
42 results. Furthermore, using the migration transects, both methods are sufficiently computationally
43 efficient to allow large scale DGVM simulations with migration.

44 **1. Introduction**

45 A large suite of dynamic global vegetation models (DGVMs) is currently used to simulate the effects
46 of climate and / or land use change on vegetation and ecosystem properties. These simulations result
47 in projections (or hind-casts) of species ranges as well as changes in ecosystem properties such as
48 carbon stocks and fluxes. Examples of these DGVMs include ORCHIDEE (Yue et al., 2018), LPJ-
49 GUESS (Sitch et al., 2003), IBIS (Foley et al., 1998), (Sato et al., 2007), for a review of DGVM
50 features see (Quillet et al., 2010).

51 While most DGVM applications use plant functional types (groups of plant species with similar traits
52 and responses to environmental conditions), here we only consider applications which explicitly
53 simulate tree species, e.g. (Hickler et al., 2012). These models typically assume that species can
54 establish at any site once the environmental conditions become suitable. However, in real ecosystems
55 species need not only to establish and replace existing vegetation – the processes gap models describe
56 successfully – but they also need to have a sufficient amount of seeds at a given location to
57 successfully establish. Implicitly, current DGVMs assume that ample amounts of seeds of all species
58 are present in every location.

59 While this approach might seem reasonable in cases where the vegetation can keep up with climate
60 change (i.e. moving sufficiently fast to occupy areas which become suitable), there have been a
61 number of instances reported where a considerable migration lag occurred. For instance *Fagus*
62 *sylvatica* has been shown to have a considerable migration lag and is currently still in the process of
63 occupying its climatological optimum (Bradshaw and Lindbladh, 2005).

64 Not only for the simulation of historical species ranges is the implementation of migration into
65 dynamic vegetation models of interest. Also for the projection of ecosystem properties in the future
66 (with projected climate), migration lags might lead to uncertainties in projected ecosystem properties
67 if the wrong species community is predicted to occur at a certain site (Neilson et al., 2005). Especially,
68 given that the speed at which environmental conditions change currently is unprecedented at least over
69 the last centuries, effects of the migration lag of key species should be evaluated when projecting
70 ecosystem properties. This holds in particular for projections over several centuries. For periods of
71 less than 50-100 years ahead, which corresponds to at most a few generations of most tree species, the
72 explicit modelling of seed dispersal might be less important for simulating tree distributions, in
73 particular when taking into account the overwhelming influence of human activities.

74 Migration lags can be caused by different factors. Seed transport might only occur over limited
75 distances. But also low seed amounts and in particular long generation times can slow down
76 migration. Seed amount and generation time depend on the competition with other trees: a free
77 standing tree starts earlier to produce seeds and produces more than a tree of the same age in a closed
78 forest. The competitors, however, are also migrating, which leads to feedbacks between the species.

79 Thus, for simulations over large areas covering long time spans, species migration – consisting of a)
80 local dynamics influenced by the environment, b) competition between species, and c) seed dispersal –
81 has to be taken into account simultaneously for several species.

82 Species migration has been implemented successfully in dynamic vegetation models working on
83 smaller extents and finer scales than DGVMs typically use, e.g. forest landscape models (FLMs;
84 review in Shifley et al, 2017), such as TreeMig, (Lischke et al., 2006), Landclim (Schumacher *et al.*,

85 2004), Landis (Mladenoff, 2004), or Iland (Seidl et al., 2012) or spatially explicit individual based
86 models such as LAVESI (Kruse et al., 2018).

87 In these models, seed dispersal is modelled in a straightforward way: seeds are distributed from each
88 producing to each receiving cell with a distance dependent probability. However, transferring these
89 approaches to DGVMs is problematic, due to a number of conceptual and technical difficulties.
90 DGVMs usually operate on a coarse spatial resolution to reduce computational load and input data
91 requirements. This neglects the spatial heterogeneity within the grid cells. Additionally, and even more
92 critical for implementing migration, it leads to discretization errors: if it is assumed that the forest
93 representing the grid cell is located in the centre of the cell, the seeds cannot move far enough to leave
94 the cell (given a typical cell size of 50km by 50km or 10km by 10km). If it is assumed in contrast that
95 the simulated forest is uniformly distributed in the cell, with each time step some seeds reach the
96 neighbour cell, leading to a resolution dependent speed up of migration.

97 Also some specifics of model implementations might complicate the inclusion of migration in some
98 DGVMs. Many DGVM implementations are done in a way that for each grid cell all years are
99 simulated before the simulation of the next cell is started. This is done to minimize input-output effort
100 since the whole climate data for each cell is read in at once and it also eases parallelisation for multi-
101 core computers, since in this case each node is assigned a number of grid cells which the node
102 calculates independently of the other nodes without communication. However, for simulating seed
103 dispersal, all cells need to be annually evaluated. Additionally to the reasons mentioned before, most
104 DGVM applications use plant functional types which comprise typically species with very different
105 traits with respect to migration (e.g. dispersal vectors or seed properties). Hence introducing migration
106 would require to split up PFTs into smaller groups and to parameterise the additional properties.

107 There have been a number of attempts to integrate species migration in DGVMs (cf. Snell *et al.*, 2014,
108 and Discussion section). For example, Sato and Ise (2012) developed a DGVM where species could
109 potentially migrate between neighbouring cells with a fixed rate of about 1km/year while Snell et al.
110 (2014) simulated migration as an infection process.

111 However, to the knowledge of the authors, there is no implementation into a DGVM which allows
112 simulations with a large extent, which takes into account the migration within the grid cell and
113 includes feedbacks between all simulated species.

114 Here we present two methods to fill this gap, i.e. allow simulating species migration of several species
115 simultaneously. The methods are implemented into the LPJ-GUESS DGVM but can potentially also
116 be implemented into other DGVMs. Though they are tested here using a virtual landscape, they can be
117 applied for simulations of large areas given current computing resources.

118 **2. Methods**

119 **2.1 The dynamic vegetation model LPJ-GUESS**

120 LPJ-GUESS is a flexible framework for modelling the dynamics of terrestrial ecosystems from
121 landscape to global scales (Sitch et al., 2003; Smith et al., 2001). This DGVM consists of a number of
122 sub-modules containing formulations of subsets of ecosystem processes at defined spatial and
123 temporal scales. Similar to most other DGVMs, it requires time series of climate data (precipitation,
124 air temperature and shortwave radiation), soil conditions and carbon dioxide concentrations as input
125 and explicitly simulates vegetation cover. While it uses plant functional types in most applications,
126 some applications simulate tree species (e.g. Hickler et al., 2012; Lehsten et al., 2015). LPJ-GUESS
127 explicitly simulates canopy conductance, photosynthesis, phenology, and carbon allocation. It uses a
128 detailed individual-based representation of forest stand structure and dynamics. Each species (or PFT)
129 has a specific growth form, leaf phenology, life history and bioclimatic limits, determining its
130 performance and competitive interactions under the forcing conditions and realized ecosystem state of
131 a particular grid cell (Sitch et al., 2003). A large body of publications describes the features of LPJ-
132 GUESS in detail; here we concentrate on the changes that were applied to LPJ-GUESS version 4.0
133 (Lindeskog et al., 2013; Smith et al., 2014). To differentiate between the original version of LPJ-
134 GUESS and our extended version (where we implemented the migration module) we refer to the
135 extended version as LPJ-GM (short for LPJ-GUESS-MIGRATION).

136 **2.2 Technical implementation**

137 Standard LPJ-GUESS simulations are typically performed at a computing cluster with cells running on
138 different nodes of the cluster without any interaction of the nodes. We implemented a distributed
139 simulation using MPI (Clarke et al., 1994) with the grid cells communicating with a master process.

140 Seeds are produced potentially in each grid cell at the end of each migration year. The number of seeds
141 produced is sent to the node computing the dispersal while all nodes wait for this master node to finish
142 the calculation. This node sends the number of seeds that arrive at each grid cell back to all nodes to
143 continue the calculation.

144 Similar to the standard version of LPJ-GUESS (Sitch et al., 2003; Smith et al., 2001), in the first 100
145 years no seed dispersal is performed and all species are allowed to establish and grow without seed
146 limitation and without N-limitation to equilibrate the soil pools with carbon and nitrogen. This time
147 period is used to sample NPP given a certain N deposition and climate to subsequently equilibrate the
148 N pools of the soil and a fast spin-up of 40000 years approximated using the sampled rates of C
149 assimilation (Smith et al., 2014). After this initialisation period all vegetation is killed and succession
150 starts from a bare soil and now seed limitation is active.

151 In LPJ-GM seed dispersal is done on an annual basis which corresponds to the temporal resolution of
152 seed production. The amount of seeds produced is communicated to the master node at the end of each
153 year. The master node re-distributes seeds over the whole spatial domain according to the dispersal
154 algorithm and communicates the amounts of arriving seeds back to each grid cell. Seeds transferred to
155 the grid cells are added to the seed bank which determines establishment probability in
156 environmentally-suitable cells (environmental suitability is determined by means of environmental
157 envelopes, containing amongst others minimum survival and establishment temperatures; see; Smith et
158 al. 2001). All communications between the processes are done via MPI protocol (Clarke et al., 1994).

159 LPJ-GUESS is a gap model with the typical successional vegetation changes. To even out
160 successional based fluctuations in ecosystem properties and to be able to simulate disturbances most
161 previous applications simulate a certain number of replicate patches are simulated per grid cell. All
162 patches share the same climate but potentially differ in their successional stage due to different timing
163 of disturbances and stochastic mortality. Conceptually, each patch has a size of 1000 m² but represents
164 an area depending on the resolution of the grid cell. Patches have no spatial position with respect to
165 each other and do not interact (Smith et al., 2001). In LPJ-GM we reduced the number of patches to
166 one but achieved the representative averaging by using explicitly placed small grid cells instead of
167 statistical units (replicate patches). For each large grid cell in the climate grid we simulate a large
168 number of cells of 1km² area resulting in a more than sufficient averaging of successional stages. LPJ-
169 GUESS simulations are typically performed with patch numbers around 10 (e.g. Smith *et al.*, 2001)
170 but depending on the aim of the simulation patch numbers have been increased even to 500 (e.g.
171 Lehsten *et al.*, 2016). In our setup even with 50 km corridors (see below and Fig. 3) LPJ-GM
172 represents a 0.5x0.5 degree cell with 200 simulation cells ranging at the higher end of the patch
173 number per area compared to previous simulations.

174 **2.3 Migration processes**

175 **2.3.1 Seed production**

176 The seed production starts once the tree reaches maturity height and is scaled linearly with leaf area up
177 to maximum LAI.

178 The seed number produced per tree is calculated as the product of the maximum fecundity multiplied
179 by the proportion of the current LAI to the maximum LAI and multiplied by the area per grid cell
180 (Lischke et al., 2006). For example, the maximum fecundity of beech is 29000, the maximum LAI is 5
181 m² * m⁻² and the maturity height is 14.4 m. Hence a tree of 15m height is above the maturity height,
182 and with an LAI of 2.5 m² * m⁻² it will produce 29000*0.5/5=14500 seeds. No specific age of maturity
183 is taken into account.

184 All seeds of a species produced $S(x',y')$ at a location (x',y') within a year are available for seed
 185 dispersal. Once seeds have entered the seed bank, no further dispersal is possible (they remain in the
 186 seed bank). Though LPJ-GUESS keeps track of carbon allocated to the main plant compartments and
 187 even allocates a certain amount of carbon to seeds (which is transferred to the litter pool, the soil pool
 188 and finally the atmosphere), for simplicity we decided not to relate the seed production to the carbon
 189 accounting at this point. Allocation rules including seed production and even mast fruiting effects
 190 (synchronised strong increases in seed production e.g. similar to Lischke *et al.* 2006) could be
 191 included in the future.

192 **2.3.2 Seed dispersal**

193 The produced seeds are distributed according to

$$194 \quad S_d(x, y) = \int S(x', y') k_s(x - x', y - y') dx' dy' \quad (\text{eq. 1}).$$

195 $S(x', y')$ is the seed production, and $k_s(x - x', y - y')$ the seed dispersal kernel in euclidean
 196 coordinates. The seed distribution $S_d(x, y)$, i.e. the input of seeds in location x, y is then obtained by
 197 integrating over all possible locations x', y' for arriving at x, y .

198 Thus, the seed distribution is given by the convolution (**) of the seed production and the seed
 199 dispersal kernel:

$$200 \quad \mathbf{S}_d = \mathbf{S} ** \mathbf{k}_s. \quad (\text{eq. 2})$$

201
 202 For this study we used the seed dispersal kernel and parameterization for *Fagus sylvatica* from
 203 TreeMig (Lischke *et al.*, 2006). The seed dispersal kernel defines the probability of seeds arriving at a
 204 sink cell (x,y) from the source cell (x',y') with a certain distance $z = \sqrt{(x - x')^2 + (y - y')^2}$.

205 The kernel is specified in a polar coordinate system,

206 $k_s(z, \theta) = k_s(z|\theta)k_s(\theta)$, with the radial distance z . The seeds follow a mixture of two exponential
 207 distributions, the short and the long term dispersal, while the angular dispersion, θ , is uniform in all
 208 directions (in our case the angular dispersion θ is uniform, but if one is interested e.g. in implementing
 209 wind directions this can be changed). Thus, the radial component of the kernel is given by

$$210 \quad k_s(z|\theta) = (1 - \kappa) \frac{1}{\alpha_{s,1}} e^{-\frac{z}{\alpha_{s,1}}} + \kappa \frac{1}{\alpha_{s,2}} e^{-\frac{z}{\alpha_{s,2}}}, \kappa \in (0,1) \quad (\text{eq. 3})$$

211 while the angular term is given by

$$212 \quad k_s(\theta) = \frac{1}{2\pi} \text{ for } \theta \in [0, 2\pi] \quad (\text{eq. 4.1})$$

213

214 $k_s(\theta) = 0$ otherwise . (eq. 4.2)

215

216 The dispersal kernel is defined by the species specific values for the proportion of long distance
217 dispersal κ and the species expected dispersal distances $\alpha_{s,1}$ and $\alpha_{s,2}$ for the two kernels.

218 The species specific values for these parameters (0.99 for κ_s and 25m and 200m for the two mean
219 dispersal distances k_s for *Fagus sylvatica*) were taken from by Lischke *et al.* (2006).

220 **2.3.3 Seed bank dynamics**

221 The number of the seeds in the seed bank (i.e. the dormant seeds in the soil that can germinate in
222 subsequent years in each cell) is increased by the influx S_d of seeds according to (eq. 1), and reduced
223 by the yearly loss of germinability (caused by decay of seeds) and the amount of germinated seeds at
224 the end of each simulated year, similar to TreeMig (Lischke et al., 2006).

225 For each grid cell and each year we prescribe whether the species requires seeds to establish. By not
226 requiring seeds in some cells for establishment or not requiring seeds for establishment for some
227 species for all cells we define refugia, or in the latter case we define that the species' seeds are known
228 to be very far dispersed and hence no explicit simulation of establishment by seeds is required for this
229 species. Technically this is implemented by reading in a list for each cell containing a year from which
230 onwards a species' establishment is not limited by the availability of seeds.

231 **2.3.4 Germination**

232 LPJ-GUESS is a gap model and in the original version the number of newly established saplings only
233 depends on the amount of light reaching the forest floor (given that the cell has a suitable climate). In
234 LPG-GM we additionally limit the establishment of seedlings depending stochastically on the number
235 of available seeds. Hence the seed limitation is applied before the light limitation. The probability that
236 a species establishes is given in equation 5.

237 $\pi_{est} = S p_x \pi_{germ}$ (eq. 5)

238 Where the π_{est} is the probability of the species establishing, S is the seed number and π_{germ} is the
239 seed germination proportion. The extra parameter p_x takes (implicitly) the area of each grid cell into
240 account. In our case we fixed this parameter to 0.01 after initial testing. Hence if in a certain year 100
241 seeds are in the seed bank and the germination rate is 0.71 (value for *Fagus sylvatica*) the probability
242 of establishment is $0.01 * 100 * 0.71 = 0.71$.

243 **2.4 Enhanced dispersal simulation**

244 One way to simulate seed dispersal is to calculate the convolution of the matrix containing the seed
245 production and the seed dispersal kernel (specified in eq. 1 and eq. 3). However, evaluating the
246 convolution explicitly can be computationally expensive for seed dispersal kernels with long range.

247 **2.4.1 Fast Fourier transformation method (FFTM)**

248 An alternative is based on the convolution theorem and the Fast Fourier Transformation (FFT), a
249 technique commonly used in physics, image processing and engineering (Strang, 1994), but rarely in
250 ecology (see e.g. Shaw et al., (2006), Pueyo et al., (2008) or Powell, (2001).

251 This approach carries out the computations in the frequency domain, see Gonzales & Woods (2002).

252 Here we use the notation $F\{S\} = \int e^{-iux-ivy}S(x,y) dx dy$ to denote the two dimensional Fourier
253 transform of S and correspondingly $F\{k_s\}$ the two dimensional Fourier transform of k_s . It then follows
254 that the Fourier transform of the convolution equals the product of the Fourier transforms

$$255 F\{S ** k_s\} = F\{S\}F\{k_s\} \quad (\text{eq. 6})$$

256 Thus, it is possible to compute the convolution by applying the inverse Fourier transform to the
257 products of the Fourier transforms

$$258 S ** k_s = F^{-1}\{F\{S\}F\{k_s\}\} \quad (\text{eq. 7})$$

259 This equation must be discretized before evaluating it on a computer. The discrete Fourier transform is
260 computed using the Fast Fourier Transform (Cooley and Tukey, 1965), which has a computational
261 cost of $O(N^2 \log^2(N))$ in two dimensions. The discrete approximation of S_d is then given by

$$262 S_d = F^{-1}\{F\{S\} \odot F\{k_s\}\} \quad (\text{eq. 8})$$

263 where \odot is the element-wise (Hadamard product) multiplication of matrices.

264 Nowadays, software packages for FFT typically only compute positive frequencies. That means that
265 we have to shift the frequencies prior to the element-wise multiplication of $F\{S\}$ and $F\{k_s\}$. This is
266 illustrated in Fig.1, see also supplementary material S.2.

267

268 <Figure 1 to be placed here>

269 While this method allows including different wind distributions by changing the seed dispersal kernel
270 (as long as they are valid for the whole simulated area), it does not allow to use different seed dispersal
271 kernels at different locations, e.g. due to prevailing wind directions in valleys, due to barriers to animal
272 transport like a motorway, or due to lower transport permeability in already forested areas.

273 **2.4.2 Seed matrix shifting method (SMSM)**

274 Another way to simulate seed dispersal is to simulate the seed movement between the cells explicitly
275 by shifting the matrix containing the produced seeds by one position (repeatedly in all directions of the
276 Moore neighbourhood; i.e. the surrounding eight cells) and simulating seed transport of a certain
277 proportion of the seeds into the next cell. Each move can be viewed as an independent random
278 variable. Repeating these moves thus corresponds to a random walk process. The Lindeberg's
279 condition for sequences for sums of independent random variables ensures that the kernel will be
280 Gaussian under general conditions (Shiryayev, 2016), with the expected value given by the sum of
281 expected values for each random variable and similarly for the variance (see supplementary material
282 S.1 for a formal proof and a derivation of the parameters of the resulting normal distribution).

283 If this is done repeatedly it allows an easy implementation of spatial explicit differences in seed
284 dispersal kernel distributions, by adjusting the proportions of seeds being transported into the next cell
285 according to a similarly sized matrix containing the area roughness or permeability. By this approach,
286 barriers and even wind speeds in latitudinal and longitudinal directions can be implemented by
287 adjusting the dispersal probabilities accordingly. After the distribution of the dispersed seeds is
288 calculated, the seeds are added to the seed bank. An example calculation of the first three steps of the
289 SMSM (in the final simulation 10 steps are performed) is given in the Supplement S.3.

290 **2.5 Corridors**

291 Seed dispersal acts at a rather fine scale compared to the usual scale at which DGVMs are run (LPJ-
292 GUESS is typically run at a 0.5 to 0.1 degree longitude / latitude scale), though some regional
293 applications use finer grids (e.g. Scherstjanoi et al., 2014). Given that the average long distance seed
294 dispersal for example for *Fagus sylvatica* is 200 m, simulations at such a coarse scale will not be able
295 to capture this process.

296 As a compromise between currently available computing resources and required simulation detail we
297 choose a 1km scale at which we performed our simulations. However, even at this scale, simulating
298 large areas for example within the European continent would result in a high computational effort.

299 Given that in some areas the landscape is rather homogenous while other areas have a variable terrain
300 (or land use conditions), we test whether for homogenous landscapes it is sufficient to simulate the
301 local dynamics only in latitudinal, longitudinal and diagonal transects (i.e. north-south, east west, as
302 well as, northeast-southwest and northwest-southeast corridors) and how this will influence the
303 migration speed. The corridors are 1 grid cell wide and regularly placed in the simulation domain.
304 Their density can be chosen by defining the distance between the latitudinal and longitudinal
305 corridors.

306 Although LPJ-GM only simulates local dynamics in the cells along the corridors, the seed matrix
307 needed to be filled for the dispersal calculation using the FFTM or the SMSM algorithm. We applied a
308 nearest neighbour interpolation of the seed production before performing the seed dispersal calculation
309 (theoretical considerations show that a distance weighted average would strongly speed up the
310 migration).

311 **2.6 Simulation experiments**

312 To test our newly developed migration module we simulated the spread of a single late successional
313 species (*Fagus sylvatica*) through an area covered by an early successional species (*Betula pendula*).
314 The species specific parameters for both species are given in the Supplement S.4. All grid cells and all
315 years in the simulated area had a static climate suitable for both species. Though the simulated domain
316 is quadratic in our case it could have any shape. Each cell in the simulated domain has been simulated
317 independently (except for the influx and outflux of seeds) from each other. For one specific simulation
318 using the SMSM method we assumed differences in the dispersal ability (e.g. more or less permeable
319 areas or physical barriers) while the climate on all grid cells is still static and favourable. The dispersal
320 ability of the landscape is displayed in Fig. 2. Areas colored white have zero permeability, hence no
321 seeds can reach these areas.

322

323 <Fig. 2 placed here>

324

325 Figure 3 demonstrates the sequence of local dynamics on the corridors, interpolation of seed
326 production, seed dispersal on the entire grid and back via the seed input on the transects.

327 <Fig. 3 placed here>

328

329 Given the uniformity of the climate, there should be no variability in the migration speed caused by
330 differences in climatic conditions. We simulated the spread of *F. sylvatica* from a single grid cell in
331 the corner of the study area which represents the refugium. We tested several corridor distances
332 (between the parallel and between the diagonal corridors) for their effect on the migration speed. To
333 calculate the migration speed we first determined the migration distance. This was the distance
334 between the start point of the migration and the 95-percentile farthest point in the virtual landscape
335 where the leaf area index (LAI) of *F. sylvatica* was larger than 0.5. This migration distance was
336 subsequently divided by the simulated time elapsed since the start of the migration. To avoid founder
337 effects we neglected the points within the first 5 km of the refugium. The simulations were performed
338 over 3000 years and over an area of 100 by 100 cells of 1 km². Finally we ran one simulation where

339 we did not calculate the seed dispersal (but performed all communication between cells and one run
340 even without the communication), hence allowing us to estimate the computation time demand for the
341 seed dispersal calculation.

342 **2.7 Performance evaluations**

343 To estimate the performance of our methods against an implementation in which each grid cell
344 exchanges seeds with each other we developed a Matlab® script, since initial testing had shown that
345 such a procedure would be too slow to be implemented in LPJ-GUESS. Hence when evaluating the
346 performance differences from the script one has to bear in mind that these are calculated in a different
347 environment. However in a general sense we can see no reason why they should not reflect the
348 performance differences between the algorithms. The whole Matlab® script testing the performance
349 including the graphs is part of the Supplementary material.

350 **3. Results**

351 **3.1 Explicit seed dispersal**

352 The study comparing the performance of different migration mechanisms without the vegetation
353 dynamics, implemented in Matlab®, has shown that both the FFTM as well as the SMSM are
354 performing faster than the explicit dispersal from each grid cell to each other within the range of the
355 dispersal (last figure Supplement 2). This is especially pronounced if the area to be simulated is
356 increased. Though faster than the explicit dispersal method, the SMSM is still up to an order of
357 magnitude slower than the FFTM.

358 **3.2 FFTM simulations**

359 Using the parameterization from TreeMig in a complete (no corridors) simulation area of 100 by 100
360 grid cells with the size of 1km² each results in a migration speed of 34 m per year for *Fagus sylvatica*
361 (Fig. 4).

362 <Figure 4 placed here>

363 Though the establishment is stochastic, the spread is relatively smooth. The corridor distance of 10
364 km, 20 km and 50 km results in a reduced migration rate of 26, 28 and 28 m/year (compared to a
365 simulation without corridors), respectively (Fig. 4, lower three rows of panels). While in the
366 simulation without corridors the variability of the migration speed is relatively low (dots under the red
367 line in upper left panel of Fig. 4), this variability is strongly increased when corridors are simulated.
368 This is caused by *F. sylvatica* migrating along the diagonal, reaching the end point of the diagonal and
369 then migrating along the longitudinal and latitudinal corridors into cells which have actually a shorter
370 distance to the refugia than the endpoint of the diagonal.

371 The calculation time per grid cell in the whole area (range for which the seed dispersal is computed) is
372 increased by 12% by simulating the FFTM, but by using the corridors it is reduced to 36%, 22% and
373 12%, compared to simulating the full area (Tab. 1, col. 7). The proportion of computation time used
374 to perform the FFTM increases from 11% without corridors to 18%, 29% and 29% for simulations
375 with corridors every 10, 20 and 50 km. This estimate only includes the required time for computing
376 the FFT-based seed dispersal since the control run without seed dispersal still contained all
377 communication between cells. For the control run seeds were produced and send to the master but the
378 master did not compute the seed dispersal, though still communicated with all other nodes to allow a
379 fair assessment of the computation time demand of the two methods (see Tab. 1). An additional run
380 without any communication resulted in a computation time similar to the run with communication.

381 **3.3 Shifting seed simulations**

382 Initial testing of the probability parameter for the SMSM suggested a value of $p=5 * 10^{-7}$ to generate a
383 migration speed comparable to the migration speed for the FFTM based on the TreeMig
384 parameterization. Using the derivation presented in supplement 2 it is possible to calculate this
385 parameter for a Gaussian dispersal kernel. One can approximate any dispersal kernel by adding several
386 Gaussian kernel, however this would increase calculation time since the SMSM would have to be
387 performed several times. Therefore we decided to choose a parameter for the SMSM approximating
388 the migration speed rather than the seed dispersal kernel used in Lischke *et al.* (2006). This resulted in
389 a migration speed of 39 m/year for the filled area and 27m/year respective 29 m/year and 30m/year for
390 the 10 km, 20 km and 50km corridors (Fig. 5).

391 <Figure 5 placed here>

392 Similarly to the FFTM simulations, the migration speed is reduced (see table 1 for a summary). Also
393 comparable to the FFTM based seed dispersal computation, calculation time per grid cell in the whole
394 area (range for which the seed dispersal is computed) is increased by 16% by the simulation of
395 dispersal, but reduced to 35%, 19% and 11% by using the corridors. The proportion of calculation
396 time spend for simulating the seed dispersal is comparable to the proportion using the FFT, it is 16%,
397 19%, close to 23% and 32% (see Tab. 1).

398 Since the SMSM allows adjusting the probability depending on the seed transport permeability of the
399 terrain we also simulated the migration within a non-homogenous dispersal area. The results of this
400 simulation are displayed in Fig 6.

401

402 <Figure 6 placed here>

403 Though all cells of the virtual landscape have a similar climate, some cells will never be occupied (see
404 Fig. 6) because the seeds are not able to reach them (which might not be reasonable for real world
405 simulations but demonstrates the method). Migration speed is different in different parts of the
406 simulated area.

407 <Table 1 placed here>

408

409 **4. Discussion**

410 To our knowledge, in our study for the first time (tree) species migration is implemented in a DGVM
411 in a way that allows simulations of simultaneously migrating and interacting species for large areas.

412 **4.1 Performance of new migration methods**

413 The presented new methods for simulating migration in DGVMs show a promising performance in
414 different aspects.

415 The first is the gain of efficiency by the FFTM and the SMSM methods as compared to the traditional,
416 straightforward approach to evaluate the seed transport from each cell to each other (last Fig in S.2). A
417 two dimensional FFT can be obtained by successive passes of the one dimensional FFT, hence the
418 complexity will be the one-dimensional complexity squared (Gonzalez and Woods, 2002). The
419 computational complexity for the FFTM is $O(N^2 \log^2(N))$ for a $N \times N$ grid discretizing the seed
420 distribution, while the complexity of the direct implementation of the convolution approach in the
421 SMSM is $O(2KRN^2)$ for a $N \times N$ grid discretizing the seed distribution and $R \times R$ kernel with K
422 being the number of iterations of the SMSM (for the derivation see supplementary material S.1). This
423 can be computationally comparable to the FFTM for kernels with short range of R . Secondly,
424 simulating the local dynamics only along the corridors instead of in the full area resulted in a similar
425 migration pattern, and the simulated migration speed is similar to that of the simulation with full grid
426 cell cover (though it is slower, caused by the stochasticity of the establishment, see table 1), but needs
427 much less computing time (reduction of 88% for the corridors every 50km).

428 **4.2 Comparison of the two dispersal methods**

429 In this study we present two alternative methods for simulating dispersal, which differ in their
430 properties. While the FFTM allows any type of seed dispersal kernel, the SMSM corresponds to a
431 normal distribution kernel. Although other shapes of dispersal kernels can be approximated by
432 weighted sums of normal distributions, of which each of them has to be simulated by an own SMSM,
433 which will cause strong increases in computational demand.

434 On the other hand, the advantage of the SMSM lies in its ability (contrary to the FFTM) to modify the
435 parameters of the seed dispersal kernel spatially, depending on the terrain. If instead of applying a
436 single permeability for all directions, a different permeability is applied for each of the 8 directions
437 (e.g. north, northeast, east, etc.) this method also allows a spatially explicit consideration of wind
438 directions (which is not possible for the FFTM, as it relies on a universal kernel applied to the entire
439 area). Hence, depending on the aim of the analysis either one or the other or a combination of the
440 algorithms is most suitable.

441 While not implemented here, it should be theoretically possible to use the FFTM (preferably with
442 corridors) for some homogenous parts of the simulated area and the SMSM for the remaining part in a

443 single simulation. As long as the seed donor areas for both methods are exclusive, and the areas in
444 which the seeds are allowed to disperse overlap at least with the width of the kernel, we can see no
445 reasons why this should not be feasible.

446 **4.3 Comparison to other approaches**

447 Our new species migration submodule FFTM uses for the first time an algorithm based on Fast Fourier
448 Transformation to simulate dispersal in a DGVM. FFTM is due to its efficiency one of the
449 “workhorses” in mathematics, physics and signal processing (Strang, 1994). In ecology, there have
450 been a few applications using FFTs to simulate dispersal of pollen (e.g. for risk analysis, Shaw et al.
451 (2006), seeds (Pueyo et al., 2008) or even in a course compendium (Powell, 2001)), but not as a
452 standard technique in DGVMs.

453 The SMSM, in turn, mimics the seed transport process itself in a simple and straightforward way,
454 which to our knowledge has also not been implemented in DGVMs either.

455 Both approaches are combined with features of modelling species migration that are already used in
456 other dynamic vegetation models (cf . Snell, 2014).

457 The cellular automaton KISSMig (Nobis & Normand, 2014), e.g. simulates the spread of single
458 species driven by a spatio-temporal grid of suitability, and by transitions to the nearest neighbour cells,
459 which is similar to one iteration in the SMSM. The suitability based models CATS (Dullinger *et al.*,
460 2012) or MigClim (Engler and Guisan, 2009) simulate a simple demography of single species and
461 explicitly the spread based on a seed dispersal kernel.

462 To also account for ecophysiology, the CATS model was combined with LPJ-GUESS in a post-
463 processing approach (Lehsten *et al.*, 2014) which used a spatio-temporally explicit suitability
464 estimated from LPJ-GUESS simulated productivity of a single species, assuming the presence of the
465 other species. This suitability was subsequently used within CATS to simulate migration spread rates.
466 Such a post-processing approach however does not include interactions between several migrating
467 species.

468 Forest landscape models have been developed to integrate such feedbacks between species as well as
469 dispersal (He et al., 2017; Shifley et al., 2017). These models simulate local vegetation dynamics with
470 species interactions, and dispersal by explicit calculation of seed or seedling transport probabilities
471 with dispersal kernels of different shapes (e.g. LandClim (Schumacher *et al.*, 2004), Landis
472 (Mladenoff, 2004), Iland (Seidl et al., 2012)). To capture spatial heterogeneity, they run at a
473 comparably fine spatial resolution (about 20-100m grid cells), allowing only the simulation of
474 relatively small areas due to computational demands.

475 To overcome such computational limits, several approaches for a spatial upscaling of the models have
476 been put forward. For example, the forest landscape model TreeMig can operate at a coarser resolution
477 (grid cell size 1000m) because it aggregates the within-stand- heterogeneity by dynamic distributions
478 and height classes (Lischke *et al.*, 1998), which allows applications at a larger scale, e.g. over entire
479 Switzerland (Bugmann *et al.*, 2014) or on a transect through Siberia (Epstein *et al.*, 2007). Another
480 upscaling of TreeMig was achieved by the D2C method (Nabel, 2015; Nabel and Lischke, 2013)
481 which simulates local vegetation dynamics only in a subset of cells that are dynamically determined as
482 representative for classes of similar cells. This method led to a computing time reduction of 30-85% as
483 compared to the full simulation similar to our transect methods which resulted a computing time
484 reduction in a similar range depending on the configuration of the corridors.

485 In DGVMs, the discretization problem resulting from the need to upscale from the fine scale at which
486 migration processes act to the scale at which DGVMs work is very pronounced, because they are
487 designed to operate on very large extents (continents or the entire globe). Given the computational
488 demands of the simulations, they are therefore typically running at a coarse resolution for example 0.5
489 or 0.1 degree longitude / latitude, and simulate the vegetation dynamics at the centre of each of these
490 grid cells, assuming this point to be representative for the entire cell.

491 Snell (2014) approached the discretization problem for the DGVM LPJ-GUESS by also using a
492 reduced number of representative units (here patches) within each grid cell. She assumed that the
493 numerous replicates of the vegetation dynamics on a patch are randomly distributed over the area of
494 the grid cell. Migration within the grid cell is treated similar to an infection process, where the
495 probability of a patch becoming infected (e.g. of the migrating species being able to establish) depends
496 only on the number of already invaded patches within the grid cell. Only once a migrating species
497 managed to establish in a certain proportion of the patches of the simulated grid cell, further dispersal
498 (explicit via a dispersal kernel) into surrounding grid cells is possible. Yet, there is no spatial
499 orientation of the patches within the grid cell and all simulations in this approach are strongly
500 resolution dependent. Simulations of large areas such as continents remain computational challenging
501 with this approach.

502 Our transect approach, similarly to the approach of Snell (2014), uses smaller representative spatial
503 units, 1km-cells, for a spatial upscaling. Since these small grid cells are arranged in contiguous
504 corridors, the migration along these corridors can be simulated without or with only a small
505 discretization error. The results indicate that also the error potentially introduced by the interpolation
506 to the rest of the area is small.

507 Thus, with our approaches, we have combined several advantages of the before mentioned approaches:
508 the seed dispersal from forest landscape models, improved by the novel FFTM or SMSM and the

509 ecophysiology, structure and community dynamics of LPJ-GUESS. We furthermore found a
510 compromise between discretization and efficiency by the corridor method.

511 **4.4 Potential further improvements**

512 Despite the satisfying performance of the new methods in these first tests some aspects suggest further
513 development.

514 **4.4.1 Computation time**

515 Even with the computing time reduction by the corridor approach using a corridor of 50km distance,
516 the computing time required for the simulations including dispersal is still considerable. This is caused
517 by the number of cells on the corridors where the local dynamics is simulated being larger than the
518 number of replicates usually used in all the 1 or 0.5 degree grid cells simulated in traditional DGVMs.
519 For large-scale applications, the approach should be further optimized, e.g. by choosing corridors
520 even further apart from each other in homogenous areas and adapting the corridor density to the large
521 scale (between grid-cell) heterogeneity of the terrain. The within grid-cell heterogeneity in turn can be
522 accounted for by deriving seed dispersal permeability, that can be used in the SMSM approach.
523 Another area of improvement lies in the technical implementation of the seed dispersal algorithm. In
524 the current implementation, the seed dispersal is performed at a single cpu, while all other cpus wait
525 until they receive the seeds. There are certainly ways to perform the seed dispersal computation on
526 several nodes to decrease the waiting time. Furthermore, in multi-species simulations the dispersal has
527 to be calculated for each migrating species. In this case, the dispersal of different species should be
528 calculated on separate nodes. When evaluating the run times needed for the simulated areas in the
529 supplementary material it becomes obvious that sometimes larger areas resulted in shorter runtimes for
530 the FFTM (last Fig. in S.2). The differences are quite pronounced given that the time axis is
531 logarithmic. These decreases are caused by the effect that the calculation of a fft can be optimised in
532 case the domain has a size of 2^n .

533 **4.4.2 Migration speed reduction by corridor approach**

534 As expected, any sub-cell assumption results in discretisation errors. In our case the assumption of a
535 corridor reduced the migration speed. This needs to be taken into account when evaluating the result of
536 such studies. The design of the corridors might also not have been optimal, maybe a corridor wider
537 than a single cell might result in less decrease of migration speed. However, these types of analysis are
538 outside the scope of this study. One other aspect of using the corridors is that while a late successional
539 species (in our case *F. sylvatica*) has certainly no problems to establish below the early successional
540 species, in the case of an early successional species (e.g. *B. pendula*) migrating into an area occupied
541 by a late successional species, the corridors might decrease the migration speed even more. An early
542 successional species can only establish after sufficient light reaches the ground, either due to the
543 senescence of a tree of the established species or a disturbance event. The narrow corridors might
544 strongly limit the availability of such grid cells. However since early successional species have

545 typically a good dispersal ability, this should not influence simulations of tree migration following
546 climate change (e.g. after the last glaciation).

547 **4.4.3 Parameterisation of dispersal kernels and other plant parameters**

548 In this study the focus is on developing and testing the novel methods, i.e. we do not attempt to
549 correctly simulate the spread of *F. sylvatica* over a defined time period. The calculated spread rates are
550 well below most of the spread rates in the literature. *F. sylvatica* has been estimated to migrate with ca
551 100 m per year based on pollen analyses by Bradshaw and Lindbladh (2005). Although such estimated
552 high migration speeds could also be the result of glacial refugia located further north than assumed
553 (Feurdean et al., 2013), our estimates of the migration speeds of 20-30 m/year still seem rather low.
554 However, in this paper we aimed to implement tree migration by using the parameterisation of
555 TreeMig in a DGVM and thereby allow large scale simulations. Our estimated migration rates of 20-
556 30 m per year are very close to the migration rates estimated for this parameterisation for TreeMig by
557 Meier et al., (2012) which estimated a value of 22 m per year. Hence, though we implemented the
558 migration module into a conceptually very different model, the resulting migration rate remains
559 comparably similar.

560 To perform modelling runs estimating the migration speed of any species would require a fine tuning
561 of the, age of maturity, seed production, dispersal parameters, germination rates, and seed survival
562 (which are very rough estimates in TreeMig ;Lischke et al., 2006) to generate the observed migration
563 e.g. by comparing to migration rates based on pollen records. Unfortunately, though all of these
564 parameters are most likely strongly influencing the migration rates, they are not only hard to find in a
565 study performed with similar methods for all tree species, they are likely to be highly variable
566 depending on growth conditions and even provenance of the individual tree. However for a large scale
567 application at least the sensitivity of these parameters should be evaluated.

568 While we limited us to use the same approach as Lischke et al. (2006) starting seed production at a
569 fixed height of maturity which accounts for a developmental threshold, but also growth and thus for
570 environmental conditions, other studies used age of maturity as a trigger to start seed production,
571 which has been shown to be important to determine tree migration rates (e.g Nathan et al., 2011). As
572 the aim of this study was not a full sensitivity analysis but a study showing that a similar approach as
573 Lischke et al. (2006) results in comparable migration rates, we will implement the option to use age of
574 maturity in the next version of LPJ-GM.

575 Applications of our approach to simulate migration in the future are only suitable if the migration
576 speed is substantially faster than the migration speed that we reach for *F. sylvatica* (due to typically
577 shorter simulation period) and if the species is not typically planted, which is common practice in
578 many commercial forests where alien species a planted.

579 **4.5 Potential for applications**

580 The test simulations were performed at a virtual landscape of 100km by 100km, but eventually the
581 method is aimed to allow large scale simulations over several millennia. Regarding memory
582 requirements, this is possible of currently available hardware: Test runs with landscapes of 4000 by
583 4000 grid cells (i.e. the size of Europe) performed without technical problems at least regarding the
584 memory requirement (given 62 GB of RAM). The considerable computational costs however require a
585 relatively high amounts of computing time, which might be reduced by efforts for speeding up (due to
586 efficient parallelisation) of the FFTM (currently the FFTM is performed on a single node while the
587 remaining nodes are idle, one could use all nodes to perform the FFTM) or by even further apart
588 corridors.

589 **5. Conclusions**

590 The presented novel approaches offer high potential to simulate the spatiotemporal dynamics of
591 species which are migrating and interacting with each other simultaneously. The approaches are not
592 restricted to LPJ-GUESS, but can in principle be applied to other DGVMs or FLMs which simulate
593 seed (or seedling) production and explicit regeneration. The presented methods need to be improved in
594 terms of computing performance to allow simulations of tree migration at continental scale and over
595 paleo time scales. Our study also shows that the estimates for seed dispersal kernels for the major tree
596 species need to be revised to allow simulations of forest development for example over the Holocene.

597 **6. Author contributions**

598 VL, DL and HL designed the study, VL performed the simulations and the statistical analysis. MM
599 and EL contributed to the study design, MM also performed large parts of the coding. EL developed
600 the formal proof in Supplementary material S.1 and the computation performance related estimates in
601 the Conclusion section. All authors contributed to the writing of the article.

602 **7. Competing interests**

603 The authors declare that they have no conflict of interest.

604 **8. Acknowledgements**

605 This study was funded by the Swiss National Science Foundation project CompMig, Nr .
606 205321_163223 .

607 **9. Code and Data availability**

608 The code generating the figures in Supplementary material 2 are part of the material. The used DGVM
609 LPJ-GUESS containing the migration module can be requested from the author.

610 The data behind all figures will be published on the DataGURU server (dataguru.lu.se) with an own
611 DOI upon acceptance of the paper.

612 **10. References**

613

614 Allen, K. A., Lehsten, V., Hale, K. and Bradshaw, R.: Past and Future Drivers of an Unmanaged
615 Carbon Sink in European Temperate Forest, *Ecosystems*, 19(3), doi:10.1007/s10021-015-9950-1,
616 2016.

617 Bradshaw, R. H. W. and Lindbladh, M.: Regional spread and stand-scale establishment of *Fagus*
618 *sylvatica* and *Picea abies* in Scandinavia, *Ecology*, 86(7), 1679–1686, doi:10.1890/03-0785, 2005.

619 Bugmann, H. K. M., Brang, P., Elkin, C., Henne, P., Jakoby, O., Lévesque, M., Lischke, H., Psomas,
620 A., Rigling, A., Wermelinger, B. and Zimmermann, N. E.: Climate change impacts on tree species,
621 forest properties, and ecosystem services, in CH2014-Impacts (2014): Toward Quantitative Scenarios
622 of Climate Change Impacts in Switzerland, edited by O. (Meteoswiss) Foen., 2014.

623 Clarke, L., Glendinning, I. and Hempel, R.: The MPI Message Passing Interface Standard, in
624 Programming Environments for Massively Parallel Distributed Systems, edited by R. R. . Decker
625 K.M., Birkhäuser, Basel., 1994.

626 Cooley, J. W. and Tukey, J. W.: An Algorithm for the Machine Calculation of Complex Fourier Series
627 *Mathematics of Computation* An Algorithm for the Machine Calculation of Complex Fourier Series,
628 *Source Math. Comput.*, 19(90), 297–301, doi:10.2307/2003354, 1965.

629 Dullinger, S., Willner, W., Plutzer, C., Englisch, T., Schratt-Ehrendorfer, L., Moser, D., Ertl, S., Essl,
630 F. and Niklfeld, H.: Post-glacial migration lag restricts range filling of plants in the European Alps,
631 *Glob. Ecol. Biogeogr.*, 21(8), 829–840, doi:10.1111/j.1466-8238.2011.00732.x, 2012.

632 Engler, R. and Guisan, A.: MigClim: Predicting plant distribution and dispersal in a changing climate,
633 *Divers. Distrib.*, 15(4), 590–601, doi:10.1111/j.1472-4642.2009.00566.x, 2009.

634 Epstein, H. E., Yu, Q. Y. Q., Kaplan, J. O. and Lischke, H.: Simulating Future Changes in Arctic and
635 Subarctic Vegetation, *Comput. Sci. Eng.*, 9(4), 12–23, doi:10.1109/MCSE.2007.84, 2007.

636 Feurdean, A., Bhagwat, S. A., Willis, K. J., Birks, H. J. B., Lischke, H. and Hickler, T.: Tree
637 Migration-Rates: Narrowing the Gap between Inferred Post-Glacial Rates and Projected Rates, *PLoS*
638 *One*, 8(8), doi:10.1371/journal.pone.0071797, 2013.

639 Foley, J. A., Levis, S., Prentice, I. C., Pollard, D. and Thompson, S. L.: Coupling dynamic models of

640 climate and vegetation, *Glob. Chang. Biol.*, 4(5), 561–579, doi:10.1046/j.1365-2486.1998.00168.x,
641 1998.

642 Gonzalez, R. C. and Woods, R. E.: *Digital Image Processing*, 2nd ed., Prentice Hall., 2002.

643 He, H. S., Gustafson, E. J. and Lischke, H.: Modeling forest landscapes in a changing climate: theory
644 and application, *Landsc. Ecol.*, 32(7), 1299–1305, doi:10.1007/s10980-017-0529-4, 2017.

645 Hickler, T., Vohland, K., Feehan, J., Miller, P. A., Smith, B., Costa, L., Giesecke, T., Fronzek, S.,
646 Carter, T. R., Cramer, W., Kühn, I. and Sykes, M. T.: Projecting the future distribution of European
647 potential natural vegetation zones with a generalized, tree species-based dynamic vegetation model,
648 *Glob. Ecol. Biogeogr.*, 21, 50–63, doi:10.1111/j.1466-8238.2010.00613.x, 2012.

649 Kruse, S., Gerdes, A., Kath, N. J. and Herzsuh, U.: Implementing spatially explicit seed and pollen
650 dispersal in the individual-based larch simulation model: LAVESI-WIND 1.0, *Geosci. Model Dev.*
651 *Discuss.*, in review, 2018.

652 Lehsten, D., Dullinger, S., Huber, K., Schurgers, G., Cheddadi, R., Laborde, H., Lehsten, V., Francois,
653 L., Dury, M. and Sykes, M. T.: Modelling the Holocene migrational dynamics of *Fagus sylvatica* L.
654 and *Picea abies* (L.) H. Karst, *Glob. Ecol. Biogeogr.*, 23(6), 658–668, doi:10.1111/geb.12145, 2014.

655 Lehsten, V., Sykes, M. T., Scott, A. V., Tzanopoulos, J., Kallimanis, A., Mazaris, A., Verburg, P. H.,
656 Schulp, C. J. E., Potts, S. G. and Vogiatzakis, I.: Disentangling the effects of land-use change, climate
657 and CO₂ on projected future European habitat types, *Glob. Ecol. Biogeogr.*, 24, 653–663,
658 doi:10.1111/geb.12291, 2015.

659 Lehsten, V., Arneth, A., Spessa, A., Thonicke, K. and Moustakas, A.: The effect of fire on tree-grass
660 coexistence in savannas: A simulation study, *Int. J. Wildl. Fire*, 25(2), doi:10.1071/WF14205, 2016.

661 Lindeskog, M., Arneth, a., Bondeau, a., Waha, K., Seaquist, J., Olin, S. and Smith, B.: Implications
662 of accounting for land use in simulations of ecosystem carbon cycling in Africa, *Earth Syst. Dyn.*,
663 4(2), 385–407, doi:10.5194/esd-4-385-2013, 2013.

664 Lischke, H., Löffler, T. J. and Fischlin, A.: Aggregation of individual trees and patches in forest
665 succession models: Capturing variability with height structured, random, spatial distributions, *Theor.*
666 *Popul. Biol.*, 54(3), 213–226, doi:10.1006/tpbi.1998.1378, 1998.

667 Lischke, H., Zimmermann, N. E., Bolliger, J., Rickebusch, S. and Löffler, T. J.: TreeMig: A forest-
668 landscape model for simulating spatio-temporal patterns from stand to landscape scale, *Ecol. Modell.*,
669 199(4), 409–420, doi:10.1016/j.ecolmodel.2005.11.046, 2006.

670 Meier, E. S., Lischke, H., Schmatz, D. R. and Zimmermann, N. E.: Climate, competition and

671 connectivity affect future migration and ranges of European trees, *Glob. Ecol. Biogeogr.*, 21(2), 164–
672 178, doi:10.1111/j.1466-8238.2011.00669.x, 2012.

673 Mladenoff, D. J.: LANDIS and forest landscape models, *Ecol. Modell.*, 180(1), 7–19,
674 doi:10.1016/j.ecolmodel.2004.03.016, 2004.

675 Nabel, J. E. M. S.: Upscaling with the dynamic two-layer classification concept (D2C): TreeMig-2L,
676 an efficient implementation of the forest-landscape model TreeMig, *Geosci. Model Dev.*, 8(11), 3563–
677 3577, doi:10.5194/gmd-8-3563-2015, 2015.

678 Nabel, J. E. M. S. and Lischke, H.: Upscaling of spatially explicit and linked time- and space-discrete
679 models simulating vegetation dynamics under climate change., in *27th International Conference on*
680 *Environmental Informatics for Environmental Protection, Sustainable Development and Risk*
681 *Management, EnviroInfo 2013*, edited by B. Page, F. A. G. J. Göbel, and V. Wohlgemuth, pp. 842–
682 850, Hamburg., 2013.

683 Nathan, R., Horvitz, N., He, Y., Kuparinen, A., Schurr, F. M. and Katul, G. G.: Spread of North
684 American wind-dispersed trees in future environments, *Ecol. Lett.*, doi:10.1111/j.1461-
685 0248.2010.01573.x, 2011.

686 Neilson, R. P., Pitelka, L. F., Solomon, A. M., Nathan, R., Midgley, G. F., Fragoso, J. M. V, Lischke,
687 H. and Thompson, K.: Forecasting regional to global plant migration in response to climate change,
688 *Bioscience*, doi:10.1641/0006-3568(2005)055[0749:FRTGPM]2.0.CO;2, 2005.

689 Nobis, M. P. and Normand, S.: KISSMig - a simple model for R to account for limited migration in
690 analyses of species distributions, *Ecography (Cop.)*, 37(12), 1282–1287, doi:10.1111/ecog.00930,
691 2014.

692 Powell, J.: *Spatiotemporal models in ecology; an introduction to integro- difference equations.*, Utah
693 State University., 2001.

694 Pueyo, Y., Kefi, S., Alados, C. L. and Rietkerk, M.: Dispersal strategies and spatial organization of
695 vegetation in arid ecosystems, *Oikos*, doi:10.1111/j.0030-1299.2008.16735.x, 2008.

696 Quillet, A., Peng, C. and Garneau, M.: Toward dynamic global vegetation models for simulating
697 vegetation–climate interactions and feedbacks: recent developments, limitations, and future
698 challenges, *Environ. Rev.*, 18(NA), 333–353, doi:10.1139/A10-016, 2010.

699 Sato, H. and Ise, T.: Effect of plant dynamic processes on African vegetation responses to climate
700 change: Analysis using the spatially explicit individual-based dynamic global vegetation model
701 (SEIB-DGVM), *J. Geophys. Res.*, 117(G3), G03017, doi:10.1029/2012JG002056, 2012.

702 Sato, H., Itoh, A. and Kohyama, T.: SEIB–DGVM: A new Dynamic Global Vegetation Model using a
703 spatially explicit individual-based approach, *Ecol. Modell.*, 200(3–4), 279–307,
704 doi:10.1016/j.ecolmodel.2006.09.006, 2007.

705 Scherstjanoi, M., Kaplan, J. O. and Lischke, H. .: Application of a computationally efficient method to
706 approximate gap model results with a probabilistic approach, *Geosci. Model Dev.*, 7, 1543–1571,
707 doi:10.5194/gmd-7-1543-2014, 2014.

708 Schumacher, S., Bugmann, H. and Mladenoff, D. J.: Improving the formulation of tree growth and
709 succession in a spatially explicit landscape model, *Ecol. Modell.*, 180(1), 175–194,
710 doi:10.1016/j.ecolmodel.2003.12.055, 2004.

711 Seidl, R., Rammer, W., Scheller, R. M. and Spies, T. A.: An individual-based process model to
712 simulate landscape-scale forest ecosystem dynamics, *Ecol. Modell.*, 231, 87–100,
713 doi:10.1016/j.ecolmodel.2012.02.015, 2012.

714 Shaw, M. W., Harwood, T. D., Wilkinson, M. J. and Elliott, L.: Assembling spatially explicit
715 landscape models of pollen and spore dispersal by wind for risk assessment, *Proc. R. Soc. B Biol. Sci.*,
716 doi:10.1098/rspb.2006.3491, 2006.

717 Shifley, S. R., He, H. S., Lischke, H., Wang, W. J., Jin, W., Gustafson, E. J., Thompson, J. R.,
718 Thompson, F. R., Diak, W. D. and Yang, J.: The past and future of modeling forest dynamics: from
719 growth and yield curves to forest landscape models, *Landsc. Ecol.*, 32(7), 1307–1325,
720 doi:10.1007/s10980-017-0540-9, 2017.

721 Shiryaev, A. N.: *Probability*, 3rd ed., Springer Verlag, New York., 2016.

722 Sitch, S., Smith, B., Prentice, I. C., Arneth, A., Bondeau, A., Cramer, W., Kaplan, J. O., Levis, S.,
723 Lucht, W., Sykes, M. T., Thonicke, K. and Venevsky, S.: Evaluation of ecosystem dynamics, plant
724 geography and terrestrial carbon cycling in the LPJ dynamic global vegetation model, *Glob. Chang.*
725 *Biol.*, 9(2), 161–185, 2003.

726 Smith, B., Prentice, I. C. and Sykes, M. T.: Representation of vegetation dynamics in the modelling of
727 terrestrial ecosystems: comparing two contrasting approaches within European climate space, *Glob.*
728 *Ecol. Biogeogr.*, 10(6), 621–637, 2001.

729 Smith, B., Wärlind, D., Arneth, A., Hickler, T., Leadley, P., Siltberg, J. and Zaehle, S.: Implications of
730 incorporating N cycling and N limitations on primary production in an individual-based dynamic
731 vegetation model, *Biogeosciences*, 11(7), 2027–2054, doi:10.5194/bg-11-2027-2014, 2014.

732 Snell, R. S.: Simulating long-distance seed dispersal in a dynamic vegetation model, *Glob. Ecol.*

733 Biogeogr., 23(1), 89–98, doi:10.1111/geb.12106, 2014.

734 Snell, R. S., Huth, A., Nabel, J. E. M. S., Bocedi, G., Travis, J. M. J., Gravel, D., Bugmann, H.,
735 Gutiérrez, A. G., Hickler, T., Higgins, S. I., Reineking, B., Scherstjanoi, M., Zurbriggen, N. and
736 Lischke, H.: Using dynamic vegetation models to simulate plant range shifts, *Ecography (Cop.)*,
737 37(12), 1184–1197, doi:10.1111/ecog.00580, 2014.

738 Strang, G.: Wavelets, *Am. Sci.*, 82(May-June), 250–255, 1994.

739 Yue, C., Ciais, P., Luysaert, S., Li, W., McGrath, M. J., Chang, J. and Peng, S.: Representing
740 anthropogenic gross land use change, wood harvest, and forest age dynamics in a global vegetation
741 model ORCHIDEE-MICT v8.4.2, *Geosci. Model Dev.*, 11(1), 409–428, doi:10.5194/gmd-11-409-
742 2018, 2018.

743

744 **11. Contents of the supplementary material**

745

746 Derivation of the variance of the seed dispersal kernel for the SMSM S.1

747 Example evaluation of computation time difference between FFTM and the
748 traditional method S.2

749 In this appendix an example code for the FFTM is given together
750 with code demonstrating the required transformation of the seed
751 kernel for the FFTM

752

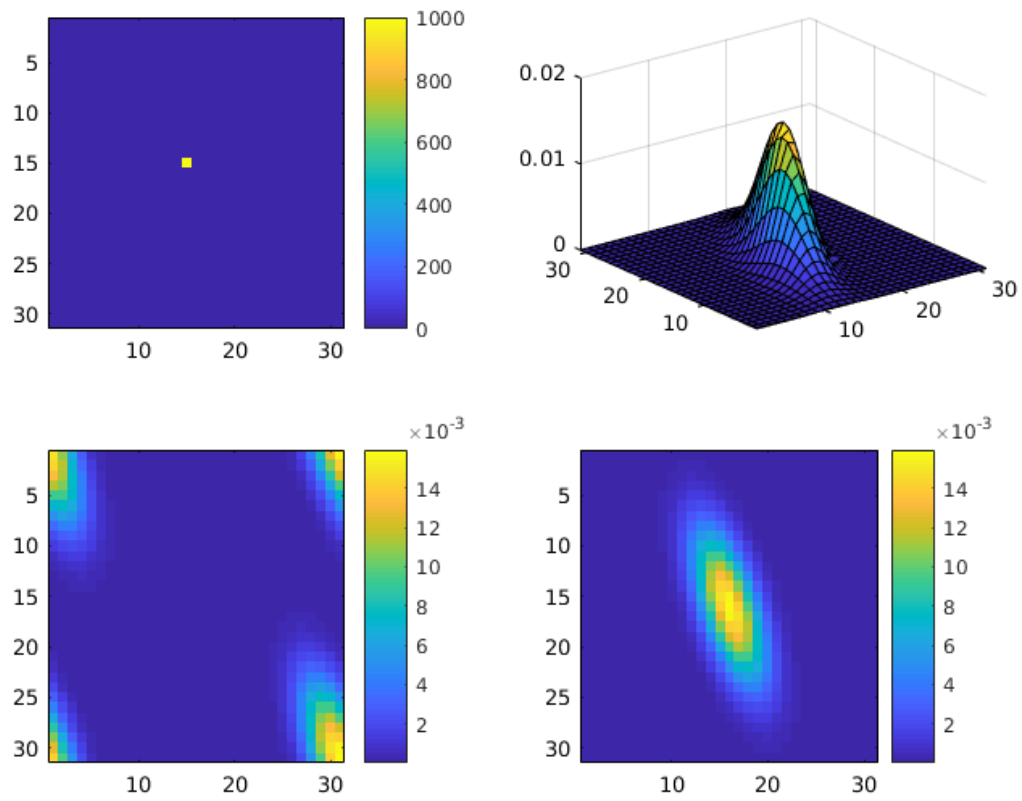
753 Example calculation of the SMSM S.3

754 Species specific parameters within the simulation S.4

755

756 **12. Figures and tables**

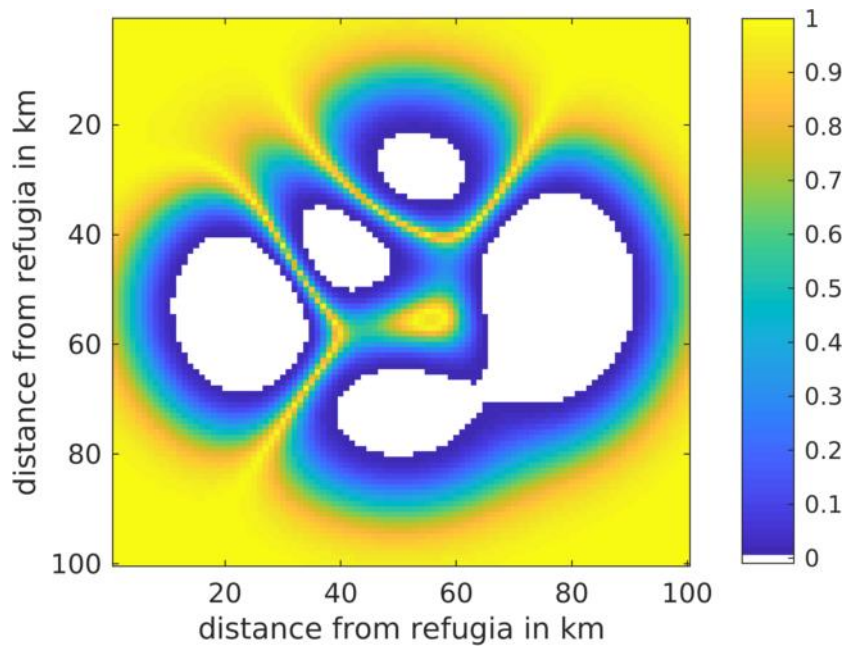
757
758



759
760 Fig. 1. Upper left panel: seed source. Upper right panel: example of a seed dispersal kernel (here a
761 non-symmetric kernel is assumed), lower left panel: transformed seed dispersal kernel, lower right
762 panel: seed distribution after convolution.

763

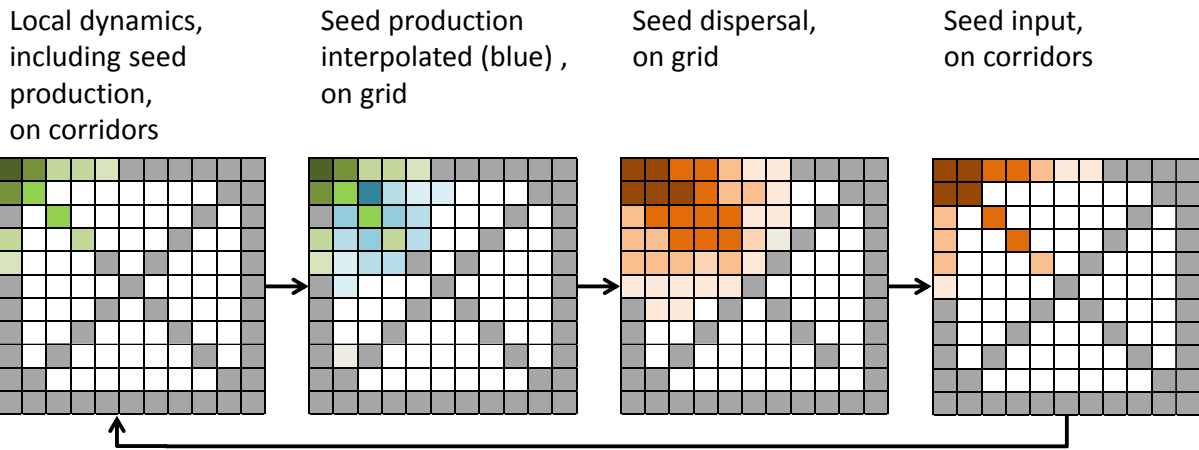
764



765
766

767 Fig. 2: Seed dispersal permeability for SMSM simulation tests. Each time the seed matrix is shifted,
768 the probability of entering the new cell (which in our test is set to $5 \cdot 10^{-7}$) is multiplied with the seed
769 dispersal permeability of the new potentially entered cell.

770

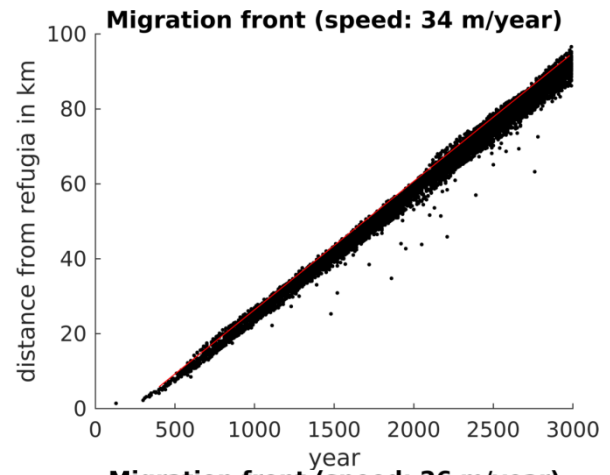
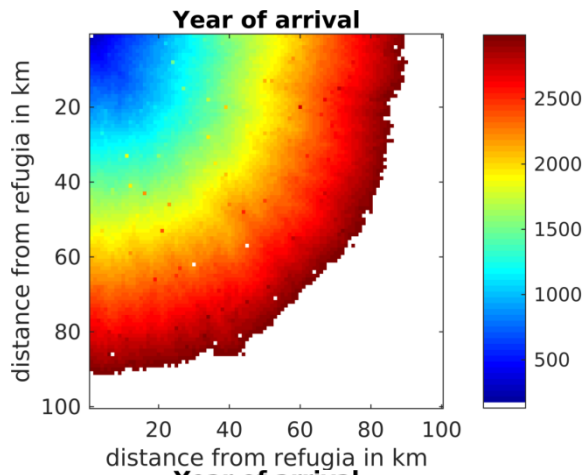


771

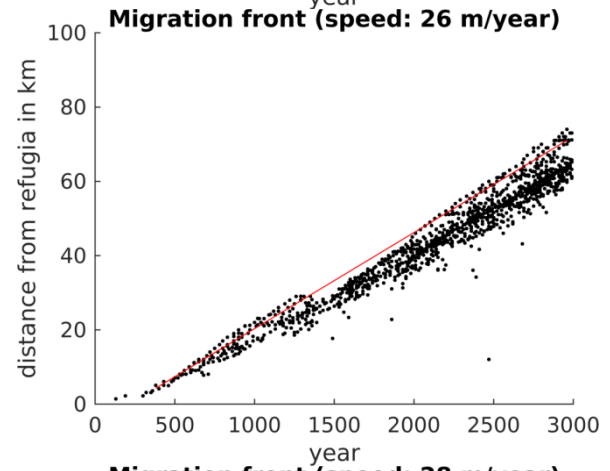
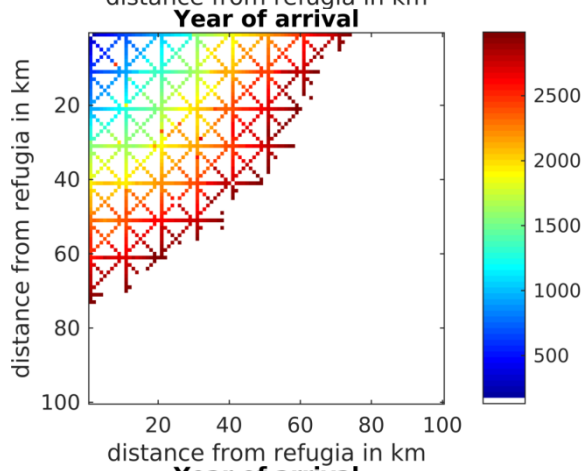
772

773 Fig. 3. Example of a simulated grid with transects (grey). In each time step the local vegetation
 774 dynamics including the seed production (green) is calculated on the transects. Then the seed
 775 production of each species is interpolated from the transects to all non-transect grid cells (blue) and
 776 then dispersed on the entire grid (brown). The seed input on the transect cell then enters the local
 777 dynamics in the next time step.

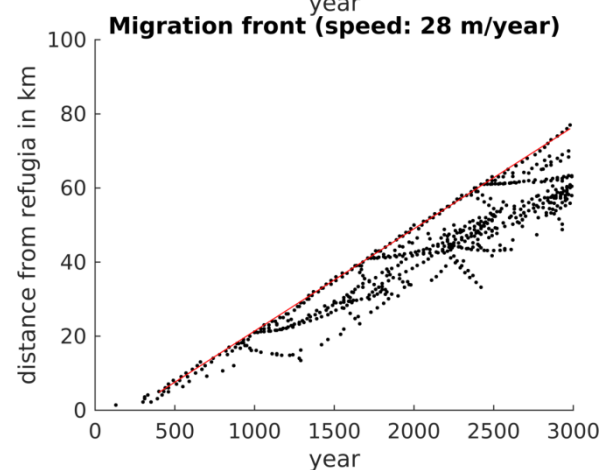
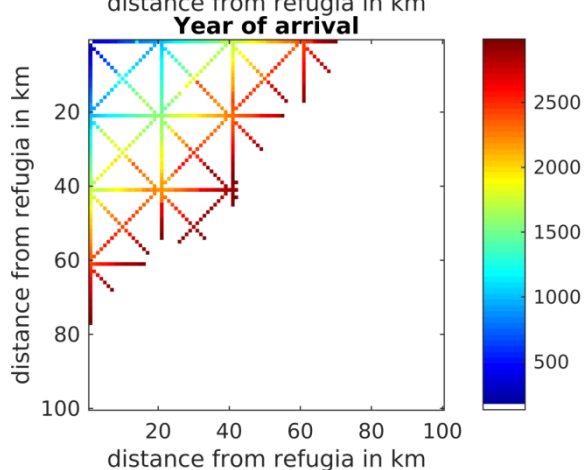
778



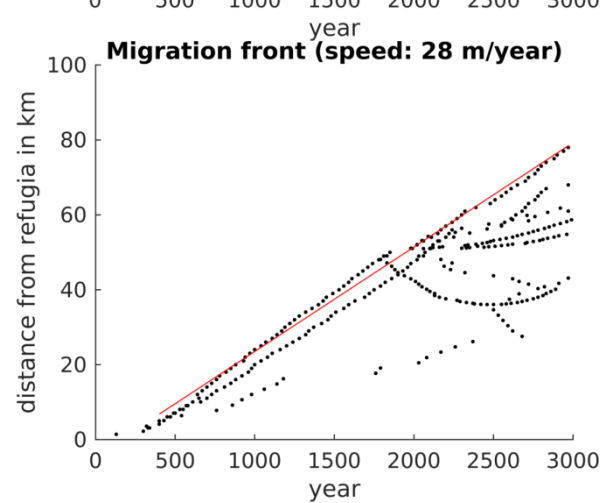
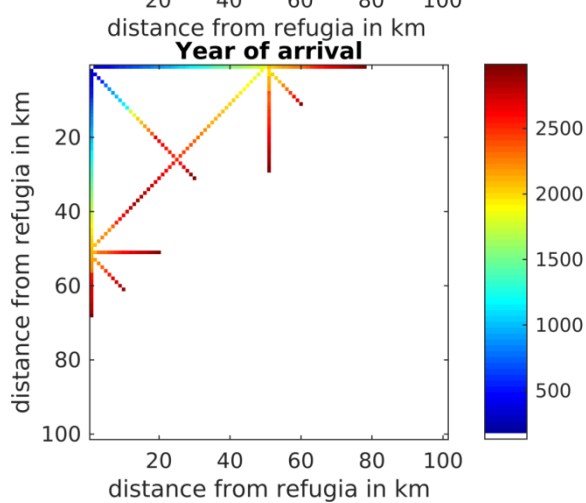
779



780



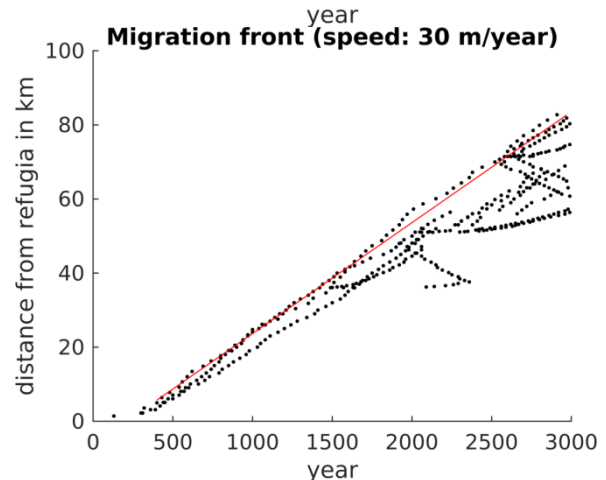
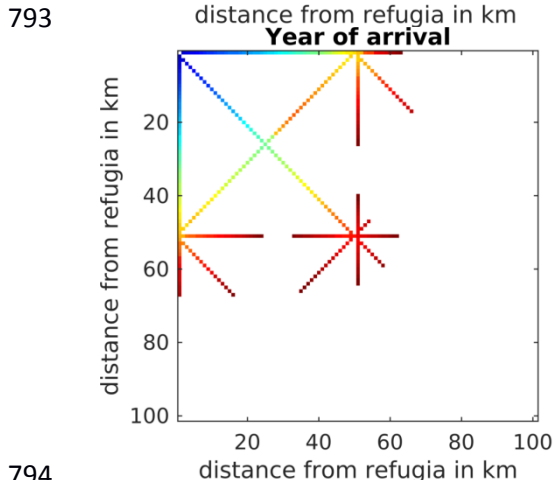
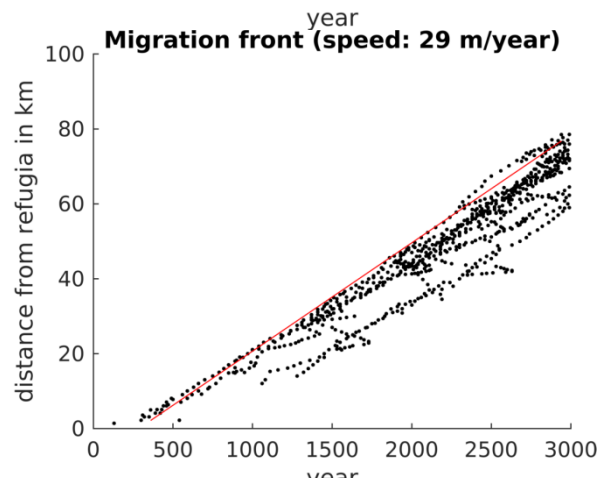
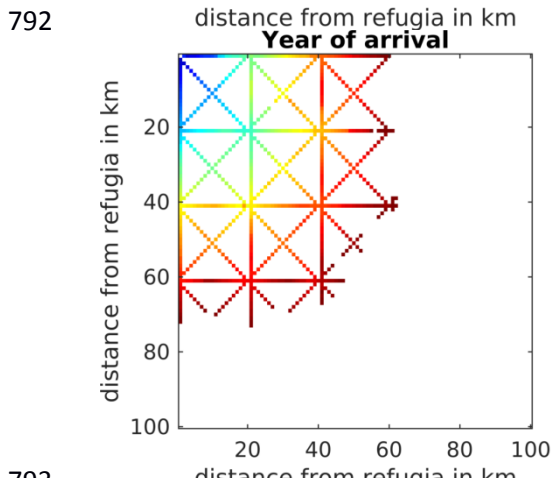
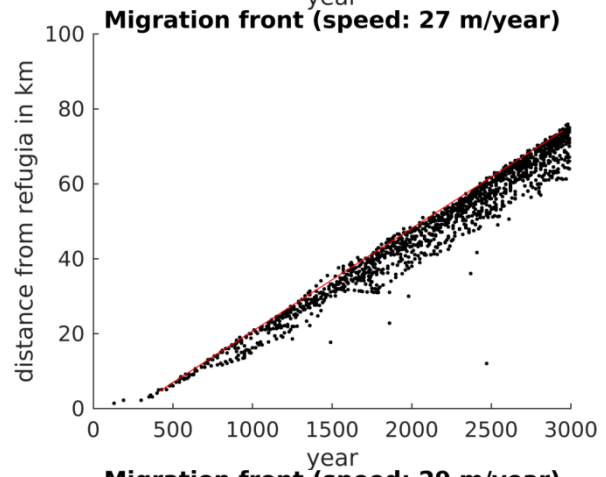
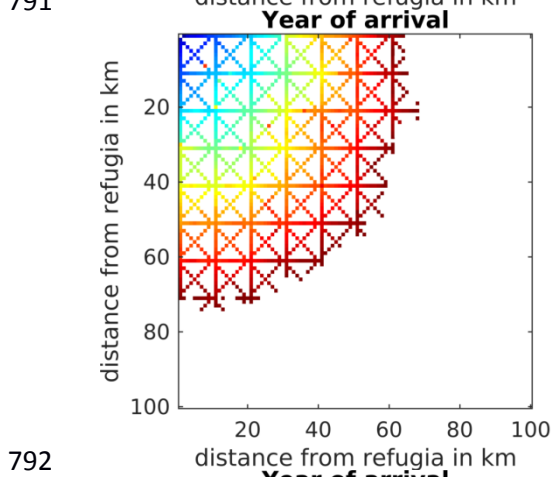
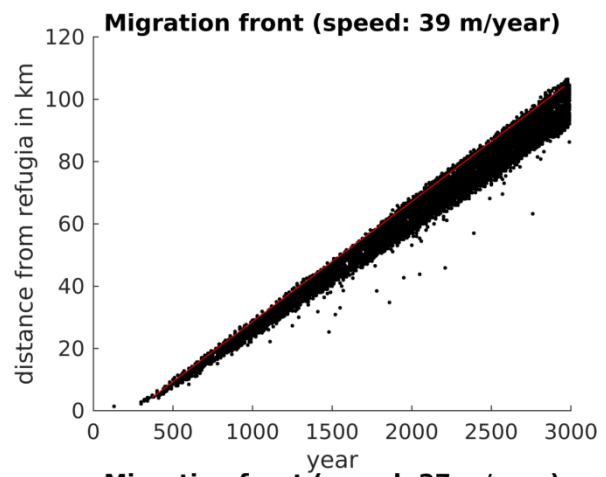
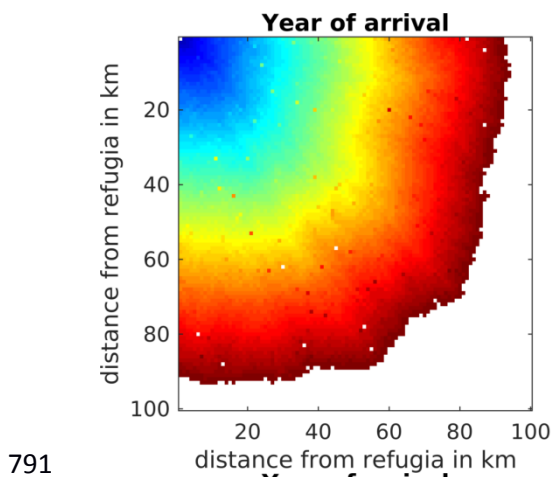
781



782

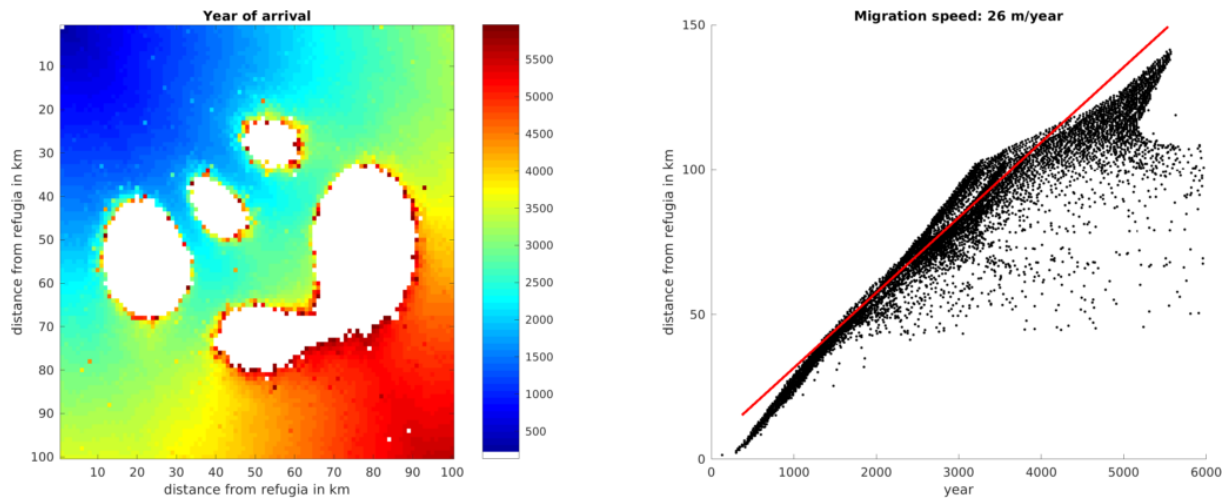
783 Fig. 4 Spread of *Fagus sylvatica* through an area of 100 * 100 grid cells with static climate using the
784 FFTM algorithm with no corridors or corridors every 10km, 20km or 50km. The left panels display
785 the time when *F. sylvatica* first reached an LAI of 0.5. *F. sylvatica* is allowed to establish freely only
786 in the upper left corner. The right panels show the distance of the grid cells with LAI 0.5 for *F.*
787 *sylvatica* from the starting point. The red line indicates the 95 percentile of the grid cells farthest away
788 from the starting point. The migration speed is calculated as slope of this line, taking only grid cells at
789 least 5 km away from the starting point into account to avoid some initial establishing effects.

790



795 Fig. 5 Spread of *Fagus sylvatica* using the SMSM through an area of 100 * 100 grid cells with
796 identical climate, using the full area (upper row of panels) or corridors every 10th, 20th or 50th cell. For
797 more explanation see Fig. 3.

798



799

800 Fig. 6 Spread of *Fagus sylvatica* using the SMSM method through an area of 100 * 100 grid cells with
 801 identical climate but probability of seed fall is set to 0.00005 multiplied with the spatially explicit seed
 802 dispersal permeability value as shown in Fig. 2. Note that we increased the simulation time to 6000
 803 years in order to have *F. sylvatica* establishing in all areas.

804

805 Table 1. Summary of migration speeds and calculation time. A corridor distance of 0 indicates no
806 corridors but an area completely filled with grid cells. The simulated grid cells column lists the
807 number of cells for which LPJ-GM calculates the population dynamics, in all simulations the
808 simulation domain (for which the seed dispersal was calculated) had a size of 10000 grid cells and all
809 simulations were performed over 3000 years. The last line lists a simulation identical to the others
810 except that no seed dispersal was calculated to allow estimating the computation time demand for this
811 operation.

Seed dispersal mode	Corridor distance (cells)	Simulated grid cells (corridor cells)	Migration speed, m/year	Computation time (CPU h)	Comp. time change per corridor grid cell compared to sim. without dispersal (CPU h)	Total comp. time change for whole domain compared to sim. without dispersal (CPU h)	Percentage of CPU time for dispersal	Decrease due to corridor simulation
FFTM	0	10000	34	1800	+12%	+12%	11%	
FFTM	10	3330	26	650	+22%	-59%	18%	67%
FFTM	20	1765	28	400	+41%	-75%	29%	78%
FFTM	50	977	27	220	+41%	-86%	29%	88%
SMSM	0	10000	39	2000	+25%	+19%	16%	
SMSM	10	3330	27	700	+31%	-59%	19%	65%
SMSM	20	1765	29	400	+41%	-77%	23%	81%
SMSM	50	977	30	220	+41%	-86%	32%	89%
Non	0	10000	0	1600	0%	0%	0%	

812